Digital optical logic using a pulsed Sagnac interferometer switch

George Eichmann, MEMBER SPIE
Yao Li
R. R. Alfano
City College of City University of New York
Institute for Ultrafast Spectroscopy and Lasers
and
Department of Electrical Engineering
New York, New York 10031

Abstract. The use of a new Sagnac interferometer switch (SIS) to perform digital optical logic is described. The optical logic switch consists of a Sagnac interferometer with an optical nonlinear material in its loop. Both the SIS input and output logic variables are optical pulses. The output SIS state is a function of the initial mirror alignment and the state of the inducing light beam. Using various SIS interconnections, all 16 two-variable binary logic functions can be implemented. Parallel logic processing of different logic functions can be performed using a single Sagnac interferometer. Since SIS elements are cascadable, sequential operation is also possible. As an example, an implementation of the SIS optical binary full adder is illustrated. If one input is a cw analog signal and another input is an ultrafast optical pulse train, the SIS can also be used as an ultrafast optical sampling device. Conditions for proper optical sampling frequency are presented.

Subject terms: digital optical computing; optical switches; optical logic networks; nonlinear optics; interferometry.

Optical Engineering 25(1), 091-097 (January 1986).

CONTENTS

1. INTRODUCTION

For a digital computer, the fundamental element that performs all three basic functions—arithmetic and logic operations and memory—is a two-stable-state switch. It has been shown that an electronic switch has its practical switching speed under 1 ns (10^{-9} s). However, because of the high speed (femtosecond) and the large bandwidth (3×10^{12} Hz) properties of an optical beam, an optical switch is a promising canonical switching element for an all-optical digital computer.[1,2] Until now, various types of binary optical and electro-optical (e-o) switches have been proposed. For such switches, three optical binary switch state representations are often used.[3] They are (1) the orthogonal polarization states, (2) the on/off states, and (3) the $0/\pi$ phase shift states.

One example of an orthogonal polarization state switch is the polarization-modulated liquid crystal light valve (LCLV).[4] If an electric signal modulates an optical beam, then the polarization switch plays the role of an e-o birefringent plate. Another example of an orthogonal polarization state switch is a degenerate phase-conjugation mirror (DPCM).[3] For different logic input polarizations, different phase-conjugated output polarization states are obtained.

Invited Paper OT-108 received Aug. 14, 1985; revised manuscript received Sept. 5, 1985; accepted for publication Sept. 8, 1985; received by Managing Editor Sept. 23, 1985.

The second type of switch, the on/off state switch, can also be implemented in different ways, such as by the use of a variable-grating mode liquid crystal (VGMLC) device,[5] a coupled-mode e-o waveguide switch,[6] a four-wave mixing device (FWM),[7] or a spatial encoding and filtering device,[8] etc. The binary logic output values are either space encoded or angle encoded. A special type of on/off state switch is an interferometric switch. For this type of switch, two basic interference models (the two-beam and the multiple-beam) are used. A nonlinear Fabry-Perot interferometer with either the e-o or the optical feedback signals is a multiple-beam interference switch (a bistable switch).[9] A two-beam interferometric switch has also been studied. For example, construction of a guided wave interferometric modulator using an e-o Mach-Zehnder interferometer has been reported.[10] Here, one arm of the interferometer contains an e-o modulator; when voltage is applied, it adds a π phase shift to the light passing through its branch. The interference output due to this π phase change could signify either an optical logic zero or a one. Since the dimensions of the waveguide are small and the switch is cascadable, the sequential logic operations can be performed, using a large number of gates, on an integrated substrate.

As for the third type of switch, binary values are represented by zero or π phase shift of the optical output signals.[11,12]

In order to have an all-optical logic network, both the input and the output logic variables must be optical quantities. A Sagnac interferometer[13] (SI) containing an optical nonlinear material (NLM), the so-called SI switch (SIS) is an excellent candidate to be a canonical element for these optical logic networks because of its autocompensation of vibrations and its ease of alignment.[14] The purpose of this paper is to explore the feasibility of using an SIS as a fast optically controlled switch. It will be shown that, using a combination of such switches, optical binary logic networks can be formed. The SIS can also be used to perform parallel processing of different binary logic functions. This parallel processing property not only allows the reduction of the dimensions of the logic network but also enhances the system synchronization. In addition, we will indi-

cate how an ultrafast optical sampling device can be realized using an SI together with a cw optical signal and a train of ultrashort optical pulses.

2. SAGNAC INTERFEROMETER

The application of interferometric methods to measurements of physical material parameters has been widely studied. Various types of interferometers have been developed for specific use. Among these is the Sagnac interferometer,[13] designed in 1913, which is also known as a triangular-path-macro-interferometer,[15] an antiresonant ring interferometer,[16] and a beam splitter interferometer.[17] Its main application was to measure absolute rotation.[13,18] Since the invention of the laser, its use has received renewed interest. The SI has found applications in the construction of ring lasers and laser gyroscopes, in quasi-microwave reentrant junctions, in laser output coupling, in cavity dumping, and in colliding-pulse mode locking.[16,19,20] Some of the properties of the SI are summarized in this section.

Figure 1 shows a rectangular-type SI. Here, a beam splitter (BS) takes the input beam and splits it into two parts. The two beams travel in an identical closed loop, but in opposite directions, before recombining at the same beam splitter. The most important feature of the rectangular-type SI is the spatial overlap of the two counterpropagating beam paths. When it is placed on a stationary table, the two counterpropagating beam paths are identical. Thus, independent of the loop size and the input frequency, the path lengths of two interfering beams are always the same. Therefore, even with a white light source, it is not difficult to align.[15] However, when the SI rotates, according to Doppler's theory, the speed of the beam traveling in one direction will be different from that of the beam traveling in the other direction. For the two counterpropagating beams, this rotation causes the beam paths to change and the corresponding interference output intensity to change also. This change can be used to calculate the rotational angular velocity.

In practical situations, the optical components suffer from random mechanical vibrations. These vibrations cause the output interference pattern to be unstable. To stabilize an interferometer, an active feedback eletronic device is often used.[21,22] However, because of the identical path property of a rectangular SI, the low frequency vibrations are autocompensated.[14]

Consider the outputs of the SI shown in Fig. 1. There are two BS output beams: one travels counter to and the other perpendicular to the input beam. We denote these two outputs as the "retroreflected output" and the "output," respectively. For all lossless SI mirrors, these two output intensities can be expressed as

$$I_r = 2r^2t^2[1+\cos\Delta\phi_r]I_i\,, \tag{1}$$

$$I_o = [t^4+r^4+2r^2t^2\cos\Delta\phi_o]I_i\,, \tag{2}$$

where subscripts i, o, and r stand for input, output, and retroreflected output, respectively, r and t are beam splitter amplitude reflection and transmission coefficients, respectively, and ϕ represents the geometrical phase difference between two interfering beams. In the case of perfect alignment and with a 50/50 beam splitting ratio, $\Delta\phi_o=\pi$ and $\Delta\phi_r=0$. Correspondingly, $I_o = 0$ and $I_r=I_i$. Thus, the input beam is totally retroreflected. When one of the mirrors is slightly misaligned, the intensities $I_o = I_i$ and $I_r=0$ can also be obtained. However, even with perfect alignment, when an unequal beam ratio is used, I_o cannot totally vanish. On the other hand, for the retroreflected output,

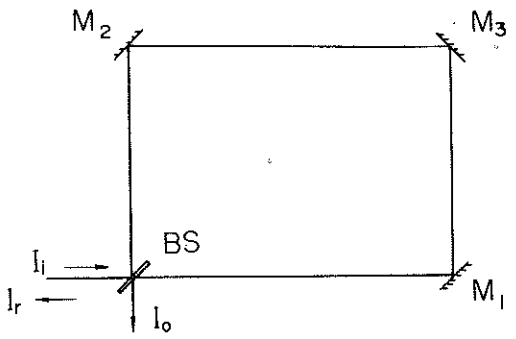

Fig. 1. Rectangular Sagnac interferometer. M, mirror; BS, beam splitter; I, intensity. Subscripts i, o, and r are input, output, and retroreflected output, respectively.

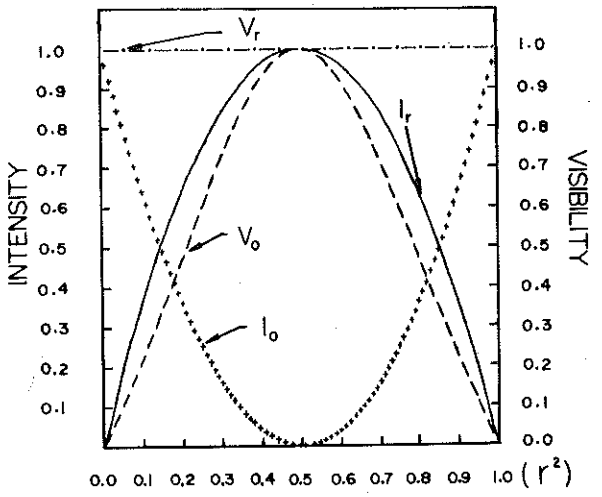

Fig. 2. Calculated curves showing the output intensities and fringe visibilities in the two output directions. V, fringe visibility; r, beam splitter amplitude reflection coefficient; I, intensity. Subscripts o and r are output and retroreflected output. Perfect alignment is assumed.

independent of the beam splitting ratio, the intensity does drop to zero. The quality of the interference fringe pattern, i.e., the fringe visibility, is defined as $V=(I_{max}-I_{min})/(I_{max}+I_{min})$. For the retroreflected output and the output signals, the fringe visibilities are

$$V_r = 1\,, \tag{3}$$

$$V_o = \frac{2t^2r^2}{t^4+r^4}\,. \tag{4}$$

Therefore, if better visibility is needed, the retroreflected output should be used. However, to couple out this output, an additional BS is needed. Thus, to get better visibility, a reduction of the output intensity is required. Figure 2 shows the theoretical output intensities and visibilities versus the beam splitter's reflection coefficient r^2 curves (assuming $\Delta\phi_o=\pi$ and $\Delta\phi_r=0$). These curves indicate that, for best results, a 50/50 BS ratio should be used.

3. SAGNAC INTERFEROMETER SWITCH

A stable binary switch forms the basic element of a digital

computer. For the construction of a binary interferometric optical switch, switch stability is one of the most important requirements. For a rectangular SI, this requirement is automatically satisfied. We will assume that to realize such a switch, an ultrafast, efficient NLM is available whose orientational relaxation time τ_0 is much faster than the inducing pulse width τ_t. For this NLM, the induced refractive index change from the linear refractive index is

$$\Delta n_{\|} = n_2 \langle E^2(z;t) \rangle , \tag{5}$$

where the symbol $\langle\rangle$ represents the time average, the subscript $\|$ is the direction parallel to the inducing light field E, and n_2 is the nonlinear refractive index. When both a signal and an inducing pulse are passed simultaneously through the NLM, an induced refractive index change $\Delta n_{\|}$ is probed. For an SI, when only one of the two counterpropagating beams undergoes this change, the output intensity of the interferometer can be expressed as (see Appendix A)

$$I_o(z;t) = B\langle E^2(z;t) \rangle \left\{ 1 + \cos \left[k_0 \ell n_2 \langle E^2(z;t) \rangle + \phi \right] \right\} , \tag{6}$$

where B is a constant, ℓ is the length of the NLM cell, k_0 is the propagation constant corresponding to the center wavelength of the input beam, and ϕ is the geometrical phase difference between two interfering beams. In order to achieve a π phase shift, a nonlinear material with a high n_2 value is required. For an isotropic material such as liquid CS_2 ($n_2 = 2 \times 10^{-20}$ mks units), achieving a π phase change requires 300 MW/cm^2 in a 1 cm long cell.[23] It has been reported that PTS polydiacetylene has a higher nonlinearity ($n_2 = 8 \times 10^{-19}$ mks units).[24] However, the recently developed semiconductor multiple-quantum-well (MQW) materials can have nonlinearity orders of magnitude higher than liquid and other bulk materials have.[25,26] In fact, 3 pJ, 82 MHz optical gates in a room-temperature GaAs/AlGaAs MQW ($n_2 = 10^{-10}$ mks units) have been experimentally demonstrated.[27] Theoretical calculations predict that even better performance can be achieved by using flatter, thinner MQW samples. In the following discussion, it is assumed that a π phase change can be induced from a high n_2 material with a resonable input power. Figure 3 shows the normalized output intensity curve, calculated from Eq. (6), for a Gaussian input pulse as a function of time. It is assumed that a 50/50 BS is used. It is clear that the output pulse shape depends on both the input pulse shape and the intensity-dependent cosine phase change. For a low initial output alignment ($\phi = \pi$), the output pulse I_o is narrower than the input pulse. However, for a high initial output alignment ($\phi = 0$), the output I_o splits into two smaller peaks with vanishing intensity at the midpoint.

An implementation of a Sagnac interferometer switch (SIS) is shown in Fig. 4. The input beams are two light pulses A and R. A cell containing NLM is asymmetrically placed into the interferometer loop so that only one of the interfering pulses can probe the induced index of refraction change. Either of the two counterpropagating pulses R_1 or R_2, can be chosen to undergo this change. To ensure that A and either R_1 or R_2 will arrive simultaneously, a delay prism D is used to adjust the temporal overlap between the two beams. Since the cell is placed asymmetrically in the loop, three pulses will not overlap simultaneously in the medium. Therefore, A does not generate a phase-conjugated signal. To obtain a larger overlap region, a small arrival angle between the two beams should be employed. When the intensity of beam A is turned off, by an adjustment of the

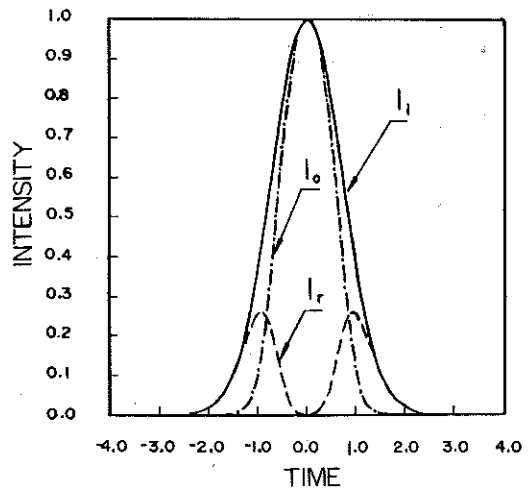

Fig. 3. Normalized time-dependent input-output relation for a Gaussian input pulse in a pulsed-mode Sagnac interferometer.

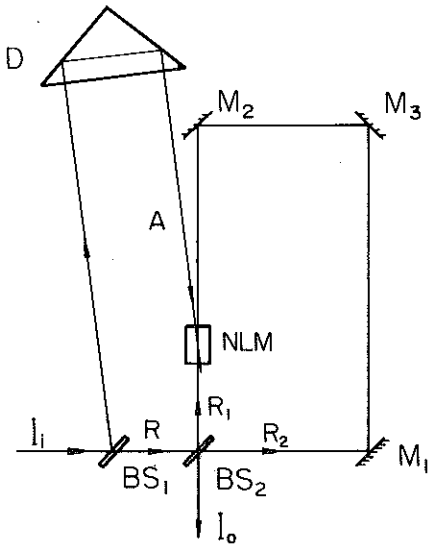

Fig. 4. Optical SI implementation of INVERTER (also denoted as a prime of the logic variable). NLM, nonlinear material; D, delay prism; I_i and I_o, input and output; A, inducing beam; R, reference beam, with subscripts 1 and 2 as clockwise and counterclockwise directions.

mirror, the interference output I_o can be placed either in an initial low energy state (in an ideal case) or in an initial high energy state. When beam A is turned on, the original output state can be switched (assuming an induced π phase change) from a low to a high state or vice versa.

This interference mechanism can serve in the role of an optical logic inverter (INV) (also denoted as a prime of the logic variable). For this optical INV, the input R serves as a reference beam, while A is the signal beam to be inverted. A similar optical INV is described in Ref. 17. There, the NLM is placed at the midpoint of the interferometer loop and is illuminated with a cw laser beam. Since there is no external inducing beam, the nonlinear phase shift is generated by the interaction of two counterpropagating beams. However, in that case, the output high state is lower than the input low state. To have an inversion between two well-defined states, a reference beam is required.

TABLE I. Two-Variable Binary Truth Table Showing All 16 Possible Two-Variable Logic Functions*

Input		Output															
A	B	1	2	3	4	5	6	7	8	9	10	11	12	13	14	15	16
0	0	0	1	0	0	1	1	0	1	0	0	0	0	1	1	1	1
0	1	0	1	0	1	1	0	1	0	0	0	1	1	0	1	1	0
1	0	0	1	1	0	0	1	1	0	0	1	0	1	1	0	1	0
1	1	0	1	1	1	0	0	0	1	1	0	0	1	1	1	0	0
		0	1	A	B	A′	B′	A⊕B	(A⊕B)′	A·B	A·B′	A′·B	A+B	A+B′	A′+B	(A+B)′	(A·B)′

*0 and 1, false and truth; ·, AND; +, INCLUSIVE-OR; ⊕, EXCLUSIVE-OR; ′, INVERSION.

4. OPTICAL BINARY LOGIC NETWORKS USING THE SIS

In this section, the formation of various binary optical logic networks using the SIS is discussed. We first describe implementations of the two-logic-variable canonical switching elements, EXCLUSIVE-OR (EOR) and AND type SISs. These switches can be shown to take more than two input logic variables. The parallel processing of different logic functions using only one SI element is discussed. Finally, as an example, a proposed implementation of an optical full adder network is described.

Table I shows all 16 possible two-variable binary logic functions. For our convenience, the table is not organized the same way as it usually appears in the logic textbooks. In the table, the symbols 0 and 1 represent false and truth values. Thus, positive logic, i.e., bright intensity true logic, is used. The first six columns contain either the constants or the single-input logic functions. The optical implementation of an INV was discussed in the previous section. Columns 7 and 8 in Table I represent the EOR and the EXCLUSIVE-NOR (ENOR) logic functions, respectively. Optical SIS implementation of EOR and ENOR is shown in Fig. 5. The logic variables, beams A and B, are the two optical logic inputs. The beam R is an optical reference pulse. The initial output intensity is chosen as a 0 (low energy) interference state. When either of the two input pulses A or B is turned on and temporally overlaps the counterclockwise reference beam at the NLM (either N_A or N_B), the reference pulse will be delayed by a half wavelength. This half wavelength delay leads the output to a 1 (high energy) state. However, when both beams A and B are turned on, the cumulative phase delay for the counterclockwise reference pulse is 2π. This delay forces the output pulse to return to the previous 0 state. Therefore, for the input logic variables A and B, the output represents an EOR logic function. On the other hand, when one of the mirrors is slightly misaligned so that 1 is obtained as the initial output, this device represents an ENOR logic function.

Instead of working with only one of the two counterpropagating beams, we can also let one logic input beam overlap the clockwise reference beam and the other logic input beam overlap the counterclockwise reference beam at the NLM. Using this approach, when two NLMs are placed symmetrically in the SI, there is no time delay between the two logic input beams. To implement these two logic functions, another alternative is to time-code the two inputs in the same NLM. The NLM is placed asymmetrically into the SI, with the arrival time for the two inputs adjusted so that one input overlaps the counterclockwise reference pulse and the other overlaps the clockwise reference pulse at the NLM.

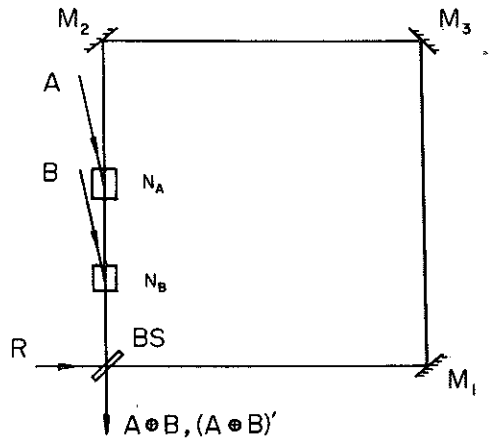

Fig. 5. Schematic diagram of an optical SI EXCLUSIVE-OR switch. Two input signals, A and B; two output signals, A⊕B and (A⊕B)′; N_A and N_B, nonlinear materials; R, reference beam.

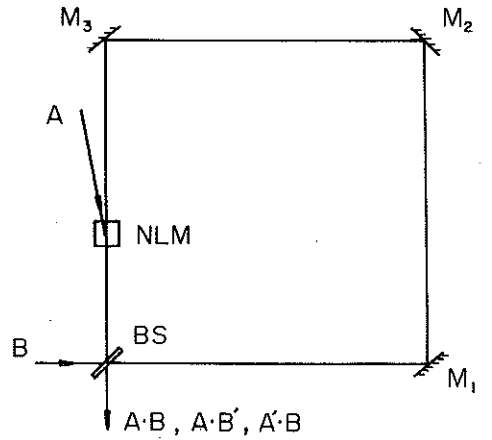

Fig. 6. Schematic diagram of an optical SI AND switch. Two inputs, A and B; three outputs: A · B, A · B′, and A′ · B.

For the optical generation of the two-variable AND function, column 9 of Table I, the optical circuit similar to the optical INV (see Fig. 4) is used. For an AND function (see Fig. 6), the reference R of Fig. 4 is replaced by the signal pulse B. Assume that the initial output, when beam A is on, is a 0. The only way to switch this output to a 1 is to have both beams A and B on. Therefore, this SIS yields a two-variable logic AND function. Here, we note that, compared to the amplitude of the signal A, the signal B is the primary input. When the value of B is a 1, depending on the initial SI mirror alignment and the value of A, the output can be either 0 or 1. However, when the value of B is 0, the output stays permanently at 0. Therefore, when 1 is chosen as the initial output, the function (A′ AND B) is realized. The function (A AND B′) can be obtained simply by interchanging the order of the two inputs.

The two-variable INCLUSIVE-OR operation, column 11 of Table I, can be realized with a BS. However, when a BS is used to combine two coherent beams, it serves in the role of an interferometer. For an INCLUSIVE-OR logic function, the phase difference between two inputs A and B should be adjusted to such a value that when both A and B are on, the interference output is the same as the output when either one of the two

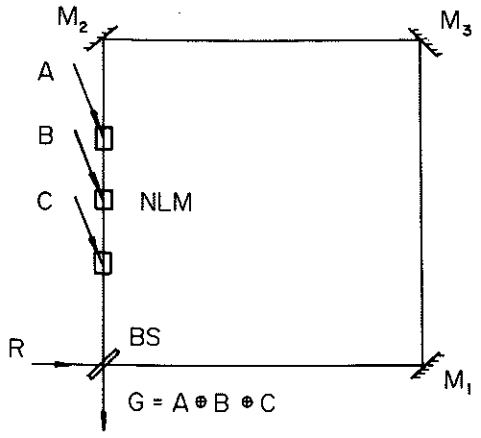

Fig. 7. Optical SI implementation of a three-variable EXCLUSIVE-OR switch. Three input signals, A, B, and C; output signal, G; reference beam, R.

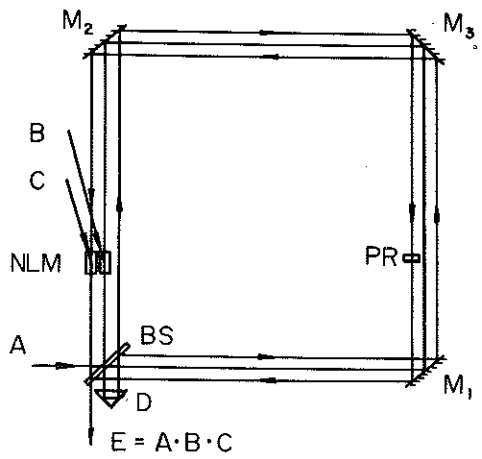

Fig. 8. Optical SI implementation of a three-variable AND switch. Three input signals, A, B, and C; output signal, E; delay prism, D; retardation plate, RP.

inputs is on. The remaining four functions, columns 13 through 16 in Table I, can also be obtained using the SIS technique. They can be synthesized using two canonical SIS elements, i.e., AND, EOR, INV, etc.

The SIS logic elements can synthesize multivariable logic functions. To illustrate this process, we present a number of examples. As a first example, consider a three-variable logic function G:

$$G = A \oplus B \oplus C, \tag{7}$$

where $\oplus$ stands for an EOR operation. To realize G, we add one more NLM and an additional signal pulse C to the original EOR switch (see Fig. 7). Again, by adjusting the SI, a 0 initial output is obtained. When one or three of the inputs are a 1, because of the odd multiple of π phase difference between two interfering beams, the output is switched from a 0 to a 1. On the other hand, when two or none of the three inputs is 1, the resultant phase difference is an even multiple of π; then, the output stays at 0. With an SIS, using similar reasoning, an N input variable EOR operation can also be performed.

As a second example, consider the generation of a three-variable AND function E:

$$E = A \cdot B \cdot C, \tag{8}$$

where the $\cdot$ stands for the logic AND. In this case, two NLM cells are used (see Fig. 8). The two NLM cells are illuminated with the signals B and C. For loop length compensation, a phase retardation plate (RP) is employed. A delay prism D, which adds a slight translational shift, is used to feed the output of the AND function (A AND B) back to the SIS. In this case, the two counterpropagating beams do not travel along the same loop. However, after traversing an identical optical distance, they recombine at a common point on the BS. After completing two round-trips, this output yields the desired AND function. In principle, this method can generate an N input AND function.

By placing the desired logic functions in displaced loops in an SI, optical parallel processing is possible. An example of this type of arrangement is shown in Fig. 9. Here, eight input (A,B,C,U,V,X,Y, and Z) and three output (O_1, O_2, and O_3) logic variables are used. When low initial output states are assumed, the three logic outputs are $O_1 = A \cdot Z$, $O_2 = B \cdot Y$, and $O_3 = C \cdot (U \oplus V \oplus X)$. In general, the number of outputs is equal to the number of primary inputs, i.e., A, B, and C in this example. The SI parallel processing not only reduces computing time but also aids in system synchronization. In SI parallel processing, when one of the mirrors suffers a small translational shift, all optical signals are identically delayed. This is an improvement over a series-connected system, in which the delays vary between different processing steps.

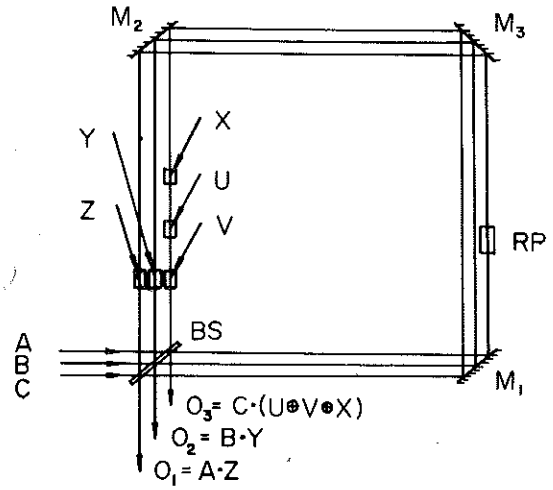

Fig. 9. Parallel processing of three logic functions using a single SI. Eight input signals, A, B, C, U, V, X, Y, Z; three output signals, O_1, O_2, O_3; retardation plate, RP.

An optical implementation of a binary full adder is considered as a final example. To add two binary number sequences, a binary full adder is usually required. The full adder logic functions are

$$S_i = A_i \oplus B_i \oplus C_i,$$
$$C_{i+1} = (A_i \cdot B_i) \oplus (B_i \cdot C_i) \oplus (A_i \cdot C_i), \tag{9}$$

where S_i is the sum of two i*th* binary number bits and C_{i+1} is the carry needed for the $(i+1)$*th* bit addition. When this full adder is used to add two binary number sequences, for the next bit addition the carry from the previous addition step is placed at

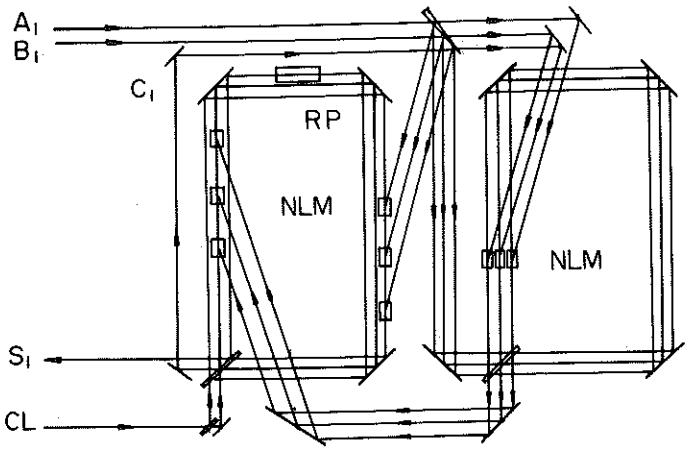

Fig. 10. Optical SI implementation of a binary full adder. A_i and B_i, two input signals (*ith* bit); C_i, *ith* carry; S_i, *ith* output of the summation; CL, clock; RP, retardation plate.

the input of the adder. The output, on the other hand, can be stored in a shift register. Consider Fig. 10 for an optical SIS implementation of the full adder. There are two SIS elements. One element (on the right side in Fig. 10) performs three AND operations. The other element (on the left side) performs two sets of three-variable EOR functions (one for generating the sum and another for generating a carry). Both SIS elements perform parallel operations. A single-bit add speed depends on the switching and the traversing time of the SIS network. To increase the speed, the size of the full adder should be reduced. Based upon the SI parallel processing concept, an optical full adder using only one SI may be implemented.

5. SAMPLING OF ANALOG OPTICAL SIGNALS USING THE SIS

So far, optical binary logic computing using the SIS has been considered. Such a system, however, with inputs that contain both digital and analog signals, can also be used as an optical sampling device. The difference between optical sampling and cavity dumping[17] is that for optical sampling a very narrow inducing (sampling) optical pulse is used. A possible optical sampler implementation is shown in Fig. 11. The NLM sample is placed asymmetrically in the SI, i.e., with unequal distances from the NLM to the BS. The primary input beam is an analog cw optical signal. In an ideal case, for perfect alignment and a 50/50 beam splitting ratio, and from a conservation of energy argument, it can be shown that the cw beam, independent of the incident intensity, will be totally retroreflected. That is, the output intensity I_o vanishes. This situation remains until an inducing pulse is incident on the NLM. For this pulse, an induced π phase change will probe two short time portions of the cw traveling wave beam. For each sampling pulse in the SI (see Fig. 12), two optical analog signal samples are obtained; i.e., the two output pulses, with the time interval equal to the traveling time difference, appear at the output O. (The cell length is assumed to be shorter than the inducing pulse width, and therefore the overlap lengths, for two counterpropagating beams, are approximately the same.) A train of N/2 sampling pulses results in a train of N analog samples. The sampling pulse period τ_s should be longer than the material relaxation time τ_o.

Since each sampling pulse generates two samples, the sampling frequency of the sampled analog signal can be twice as

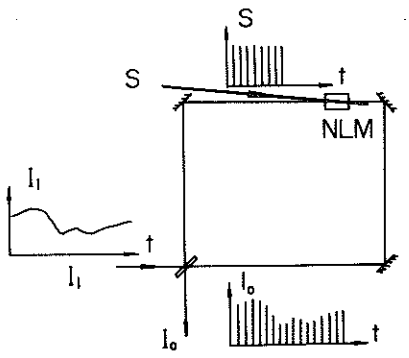

Fig. 11. SI optical analog signal sampler. I_i, optical analog input signal; S, sampling pulses; I_o, sampled output signal.

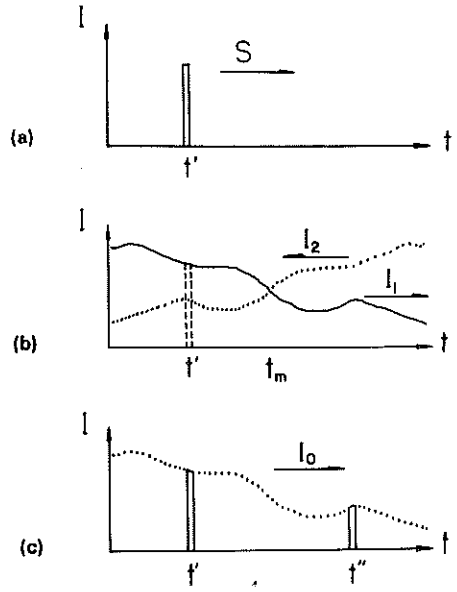

Fig. 12. Time diagram of an SI optical analog signal sampler. (a) Sampling pulse S arriving at time t_s. (b) $I_1(t)$ and $I_2(t)$, two counterpropagating analog signals in the SI; t_m, time corresponding to the midpoint of the interferometer loop. (c) I_o, resulting sampled output optical signal.

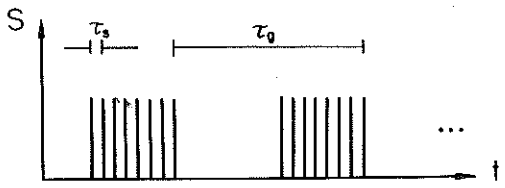

Fig. 13. Sampling pulse sequence. Sampling period, τ_s; sampling group period, τ_g.

high as the input sampling pulse frequency. For a uniformly sampled signal, the NLM should be located in the loop such that the time difference between the NLM and the midpoint of the loop is equal to $\tau_s/4$. To deduce the condition for which the output signal frequency is equal to the input sampling signal frequency, we define the parameter called the sampling signal group period τ_g (see Fig. 13):

$$\tau_g = \frac{2\ell_n}{c}, \tag{10}$$

where ℓ_n is the distance from the loop midpoint to the NLM sample and c is the velocity of light. The group period implies that there must be a time interval between every two groups of sampling pulse trains. Otherwise, the analog signal will be resampled. To obtain the largest group period, the NLM is placed immediately behind the beam splitter. The maximum number of samples N_{max} resulting from each group of the sampling pulses is

$$N_{max} = \frac{\tau_g}{\tau_s} . \tag{11}$$

When a high sampling frequency is required, the heating of the NLM due to the high repetition of the inducing laser pulse should be considered. To minimize the heating effect, an alternative SIS optical sampler realization can be employed. Here, N uniformly placed NLM cells, located asymmetrically with respect to the BS, i.e., on one side of the loop midpoint in the SI, are sampled. The advantages of this configuration are that the low repetition rate laser can be used to perform the optical high frequency sampling and each NLM is allowed to have a longer relaxation time.

6. SUMMARY AND CONCLUSION

The SIS is an attractive candidate for an all-optical digital computing element. In this paper, an autostabilized binary optical SIS has been proposed. The SIS switch-on and switch-off times depend, for $\tau_o << \tau_t$, on the switching pulse shape. The output visibility depends on the beam splitter. For best performance, a 50/50 beam splitter should be used. The constant time delay due to the loop length can be reduced and the system stability can be enhanced[14] using an integrated optics approach. Using an SIS, various binary logic functions can be implemented. It has been indicated that the SIS is suitable to parallel logic operations. The application of an SIS to fast optical sampling has been indicated. Conditions for proper sampling have been discussed.

7. ACKNOWLEDGMENT

The work reported in this paper was supported in part by a grant from the Air Force Office of Scientific Research.

8. APPENDIX A

Consider a one-dimensional sinusoidal field with a Gaussian traveling pulse envelope[28]:

$$E(z;t) = E_0 \exp\left(\frac{t-\frac{z}{c}}{\tau_t}\right)^2 \cos(w_0 t - k_0 z) , \tag{A1}$$

where c is the velocity of light, τ_t is the temporal pulse width, and w_0 and k_0 are the radian center frequency and the radiation propagation constant, respectively. Assume that this pulse is separated by a 50/50 beam splitter into two parts. One part travels clockwise while the other travels counterclockwise in an SI. The two pulses, after recombining at the BS, yield for the total electric field

$$E_o(z;t) = AE_0 \exp\left(\frac{t-\frac{z-z_1}{c}}{\tau_t}\right)^2 \times \left\{ \cos[w_0 t - k_0(z-z_1)] + \cos[w_0 t - k_0(z-z_2)] \right\} , \tag{A2}$$

where A is a constant and z_1 and z_2, with $\Delta z = z_1 - z_2$, are optical paths traveled by the two counterpropagating pulses. Here, we have used a slowly varying Gaussian envelope approximation. The corresponding time-averaged intensity is

$$I_o(z;t) = B\langle E^2(z;t)\rangle [1+\cos(k_0 \Delta z)] , \tag{A3}$$

where the symbol $\langle\rangle$ represents the time average and B is a constant. Since $\Delta z = [\ell n_2 \langle E^2(z;t)\rangle + \phi/k_0]$, with ϕ as the geometrical phase difference, we have the output intensity as in Eq. (6):

$$I_o(z;t) = B\langle E^2(z;t)\rangle \left\{ 1+\cos[k_0 \ell n_2 \langle E^2(z;t)\rangle + \phi] \right\} . \tag{A4}$$

9. REFERENCES

1. P. W. Smith, Bell System Tech. J. 61, 1975 (1982).
2. A. A. Sawchuk and T. C. Strand, Proc. IEEE 72, 758 (1984).
3. T. R. O'Meara, D. M. Pepper, and J. O. White, in *Optical Phase Conjugation*, R. A. Fisher, ed., Academic Press, New York (1983).
4. M. T. Fatehi, K. C. Wasmundt, and S. A. Collins, Jr., Appl. Opt. 20, 2066 (1981).
5. P. Chavel, A. A. Sawchuk, T. C. Strand, A. R. Tanguay, Jr., and B. H. Soffer, Opt. Lett. 5, 398 (1980).
6. J. C. Campbell, F. A. Blum, O. W. Shaw, and K. L. Lawley, Appl. Phys. Lett. 27, 202 (1975).
7. J. Fleuret, Appl. Opt. 23, 1609 (1984).
8. H. Bartelt and A. W. Lohmann, Appl. Opt. 22, 2519 (1983).
9. N. Peyghambarian and H. M. Gibbs, "Optical bistability for optical signal processing and computing," Opt. Eng. 24(1), 68 (1985).
10. H. F. Taylor, Appl. Opt. 17, 1493 (1978).
11. C. C. Guest and T. K. Gaylord, Appl. Opt. 19, 1201 (1980).
12. C. C. Guest, M. M. Mirsalehi, and T. K. Gaylord, Appl. Opt. 23, 3444 (1984).
13. G. Sagnac, C. R. Acad. Sci. 157, 708 (1913).
14. Y. Li, G. Eichmann, and R. R. Alfano. Submitted to Appl. Opt.
15. P. Hariharan and D. Sen, J. Opt. Soc. Am. 47, 528 (1957).
16. A. E. Siegman, IEEE J. Quantum Electron. QE-9, 247 (1973).
17. K. Otsuka, Opt. Lett. 8(9), 471 (1983).
18. E. J. Post, Rev. Mod. Phys. 19, 475 (1967).
19. R. Trutna and A. E. Siegman, IEEE J. Quantum Electron. QE-13, 955 (1977).
20. H. Vanherzeele, J. L. Van Eck, and A. E. Siegman, Appl. Opt. 20, 3484 (1981).
21. P. Shajenko and E. L. Green, Appl. Opt. 19, 1895 (1980).
22. A. Olsson, C. L. Tang, and E. L. Green, Appl. Opt. 19, 1897 (1980).
23. P. P. Ho and R. R. Alfano, Phys. Rev. A: 20, 2170 (1979).
24. A. Yariv, *Optical Electronics*, CBS College Publishing, New York (1985).
25. W. L. Bloss and L. Friedman, Appl. Phys. Lett. 41, 1023 (1982).
26. L. C. West and S. J. Eglash, Appl. Phys. Lett. 46, 1156 (1985).
27. J. L. Jewell, Appl. Phys. Lett. 46, 918 (1985).
28. A. Yariv and P. C. Yeh, *Optical Waves in Crystals*, John Wiley & Sons, New York (1984).